UNSTEADY AERODYNAMICS MODELLING AND ITS APPLICATION IN AEROELASTIC STABILITY ANALYSIS

Xintao Li*, Weiwei Zhang*
** School of aeronautics, Northwestern Polytechnical University, Xi'an 710072, China*

Keywords: *Reduced order modelling, vortex induced vibration, and aeroelastic stability analysis*

Abstract

An identification technique is used to construct reduced-order models (ROMs) for the incompressible flow past a circular cylinder at low Reynolds numbers. The proposed method is capable of constructing simple models for both the stable and unstable flows at the vicinity of critical Reynolds number. Linear ROMs are then validated in the time domain by comparing their harmonic forcing responses to that of full system in direct numerical simulations. Finally, the validity of linear ROMs is most clearly shown by using them for stability analysis of an elastically-mounted cylinder. The instability boundaries predicted by the linear dynamics model compare reasonably well to that of direct CFD/CSD simulations, while the computational cost can be reduced by nearly 2 orders of magnitude. Moreover, this kind of linear ROMs can also be utilized to feedback controller design and active flow control in further research.

1 Introduction

Fluid flow past a stationary circular cylinder becomes unstable beyond $Re \sim 47$ [1]: For a subcritical control parameter $Re < 47$, the flow is steady and symmetrical; while for supercritical conditions $Re > 47$, vortex begins to shed periodically at the cylinder wake, and causes the cylinder to experience unsteady aerodynamic forces. An elastically-suspended cylinder may undergo vortex-induced vibrations as a result of this unsteadiness. Under certain conditions, vortex shedding frequency may be synchronized with the vibration frequency, which is referred to as *lock-in* or *synchronization*. For a comprehensive review of the research on various aspects of vortex induced vibration one can refer to Sarpkaya [2], Williamson & Govardhan [3], and Bearman [4].

Almost all the investigations of VIV in the past have been conducted for $Re > Re_{cr}$, where Re_{cr} is the critical Reynolds number for a stationary cylinder. However, recent studies by Cossu & Morino[5] and Mittal &Singh[6] indicate that vortex shedding and self-excited vibrations of the cylinder are possible for $Re < Re_{cr}$ .Cossu & Morino conducted a global stability analysis of the aeroelastic system and found that Re_{cr} for a cylinder with fluid-to-solid density ratio larger than 1/70 is less than half that of the stationary structure case. Mittal & Singh investigated vortex shedding of an elastically mounted cylinder at subcritical *Re* by using direct numerical simulation method. They found that self-excited oscillations, accompanied by vortex shedding, are possible at *Re* as low as 20. However, direct numerical simulation of vortex induced vibrations is often insufficient in itself to address complex physics and is far too computationally expensive to be used in various multi-disciplinary settings, including control model synthesis, multi-variable optimization, and stability prediction (Lucia et al. [7]).

In the present work, we focus on constructing simple, linear aerodynamic models for the cylinder wake flow, which are useful for aeroelastic stability analysis of VIV at low Reynolds numbers, and which can also be utilized for feedback controller design in future research. Based on such linear models, computational cost of aerodynamic loads can be reduced significantly and linear control theory can be used to design robust controllers, which can give rise to improved closed-loop performance.

The two most used Reduced-Order methods are: The proper orthogonal decomposition (POD) and system identification method. POD provides a tool to construct a model based on an optimal basis required to represent a dynamical system. It has been successfully applied to many engineering and scientific problems[8-13]. For system identification method, both the integral model, such as the Volterra series, and the difference model, such as the autoregressive with exogenous input (ARX) model can be used. The fist-order Volterra series model and ARX model are linear models in which the aerodynamic load is proportional to the structural motion with the assumption of small-amplitude vibrations. In our research group, ROMs based on ARX have been applied to aerodynamics modelling, aeroelastic stability analysis and controller design [14]. Once the model is identified, it is used in place of the CFD solver in the coupled aeroelastic system to predict the structural response.

However, the reduced-order method mentioned above are mostly applicable to stable flows. For unstable flows, Illingworth [15] have pointed out that this is challenging for two reasons: First, the impulse response of an unstable system is unbounded, meaning that some standard techniques (such as balanced truncation) cannot be used; second, the growing amplitudes of the unstable modes will ultimately give rise to nonlinear, limit-cycling state, which is certainly not linear.

In this paper, we proposed a reduced-order modeling technique for the unstable flow past a circular cylinder. The idea is to perform data training on the steady-state base flow in the linear regime. then the ROMs are validated in the time domain by comparing their predicted time responses with that of direct numerical simulations. At last, the ROMs are utilized for stability analysis of an elastically-suspended cylinder.

2 Numerical method

2.1 Navier-stokes equations

The full compressible Navier–Stokes equations are utilized to simulate the essentially two-dimensional incompressible laminar flow past a circular cylinder at low Reynolds numbers. The Mach number is very small, and is taken to be Ma=0.1.The integral conservation governing equations are given as follows:

$$\frac{\partial}{\partial t}\iint_{\Omega}\boldsymbol{Q}dV+\oint_{\partial\Omega}\boldsymbol{F}(\boldsymbol{Q},\boldsymbol{V}_{grid})\cdot\vec{\boldsymbol{n}}dS=\oint_{\partial\Omega}\boldsymbol{G}(\boldsymbol{Q})\cdot\vec{\boldsymbol{n}}dS \tag{1}$$

The popular cell-centered finite volume method is used in our numerical simulations. The spatial discretization is performed on a standard collocated grid using Ausm+-up scheme. Dual-time stepping method is chosen for time integration. A no-slip wall boundary condition is applied to the cylinder surface. The far field boundary is assigned a non-reflective boundary condition to ensure that the disturbance generated by the object is not returned within the flow field. Fig.1 depicts the domain discretization with a close up view of the hybrid grid used in this study near the inner boundary. Note in particular a fine mesh closer to no-slip boundaries encompassing the circular cylinder.

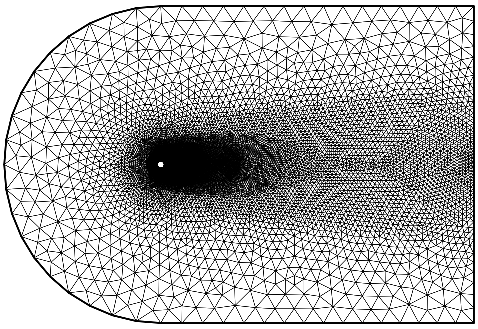

(a)

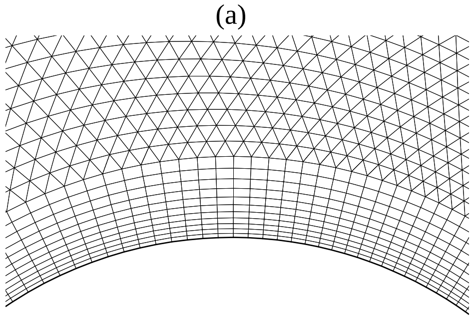

(b)

Fig.1. (a) Hybrid grid used in this paper, (b) close-up view of the hybrid grid

2.2 Cylinder motion equation

The rigid cylinder is free to vibrate in the transverse direction and the governing equation of cylinder motion is:

$$\ddot{h}+4\pi F_n\zeta\dot{h}+(2\pi F_n)^2 h=\frac{2C_L}{\pi M} \qquad (2)$$

Here， ζ is the structural damping coefficient, which is set to zero in this study. The non-dimensional natural frequency and non-dimensional mass of the cylinder are defined as $F_n = f_n \mathrm{D}/U_\infty$ and $M = 4m/(\pi\rho D^2)$ where f_n is the natural frequency, m is the actual mass of the oscillator per unit length and ρ is the density of the fluid. $\ddot{h}$, $\dot{h}$ and h denote the normalized acceleration, velocity and displacement of the cylinder in cross-flow direction. The plunging displacement and velocity of circular cylinder are normalized by D and U_∞ . $U^* = 1/F_n$ is defined as the reduced velocity. A loosely coupled solution algorithm based on CFD simulation in the time-domain is employed to solve the nonlinear FSI problems[16]. This algorithm only needs to solve the aerodynamic loads once at each physical time step .

3 Unsteady aerodynamics modeling for FSI

We are interested in finding linear models for the cylinder wake flow directly from simulation data. For subcritical Re, the flow is stable, linear models can be identified directly. However, it is difficult to find a linear model for the unstable flow at supercritical conditions $Re > Re_{cr}$ .In this paper, we proposed a method for constructing reduced-order models for unstable flows by performing data training on the steady-state base flow. we believe that the flow lies in linear dynamics in the initial develop stage from base flow to finally nonlinear limit-cycle state.

3.1 Reduced-order modeling method

Signal design is the key element in dynamics modelling. The frequency coverage of the training signal should include the frequencies of the modes that need to be excited. The training amplitude should not be too large, otherwise, the aerodynamic responses would become nonlinear. In this paper, a chirp signal with a broad band non-dimensional frequency regime [0.04,0.20] is used for data training , as shown in fig.2.

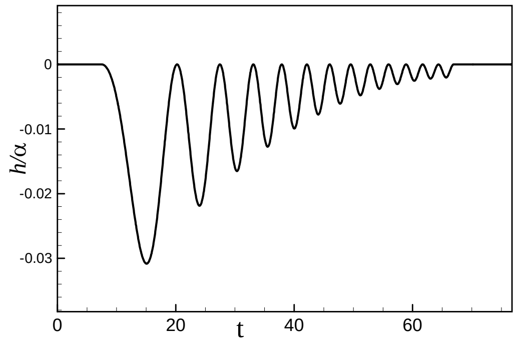

Fig.2. Training signal

The flow is perturbed by this prescribed plunge or rotational motion of the cylinder and the aerodynamic responses can then be computed by the CFD solver proposed in §2. The discrete-time-difference-equation is used to find a linear map between the input and output of the system, shown as follow:

$$\boldsymbol{y}_a(k)=\sum_{i=1}^{na}\boldsymbol{A}_i\boldsymbol{y}_a(k-i)+\sum_{i=1}^{nb\text{-}1}\boldsymbol{B}_i\boldsymbol{u}(k-i) \qquad (3)$$

Where $\boldsymbol{y}$ is the output vector of the system, $\boldsymbol{u}$ is the input vector of the system. A_i and B_i are the constant coefficients to be estimated, na and nb are the delay orders determined by the user. For the current one-input-one-output model, $\boldsymbol{u}=[h]$ or $\boldsymbol{u}=[\alpha]$, and $\boldsymbol{y}=[C_L]$.

We define a state vector $\boldsymbol{x_a}(k)$ as follow:

$$\begin{aligned}\boldsymbol{x}_a(k)=[&y_a(k-1),\cdots y_a(k-na),\\ &u(k-1),\cdots,u(k-nb+1)]^{\mathrm{T}}\end{aligned} \qquad (4)$$

Then the state–space form for the discrete–time aerodynamic model can be described as:

$$\begin{cases}\boldsymbol{x}_a(k+1)=\tilde{\boldsymbol{A}}_a x(k)+\tilde{\boldsymbol{B}}_a\boldsymbol{u}(k)\\ \boldsymbol{y}_a(k)=\tilde{\boldsymbol{C}}_a\boldsymbol{x}(k)+\tilde{\boldsymbol{D}}_a\boldsymbol{u}(k)\end{cases} \qquad (5)$$

To couple with the structural equations, the discrete-time state-space equation is then converted into the continue-time state-space form, as shown in Eq. (6):

$$\begin{cases}\dot{\boldsymbol{x}}_a(t)=\boldsymbol{A}_a\boldsymbol{x}_a(t)+\boldsymbol{B}_a\boldsymbol{u}(t)\\ \boldsymbol{y}_a(t)=\boldsymbol{C}_a\boldsymbol{x}(t)+\boldsymbol{D}_a\boldsymbol{u}(t)\end{cases} \qquad (6)$$

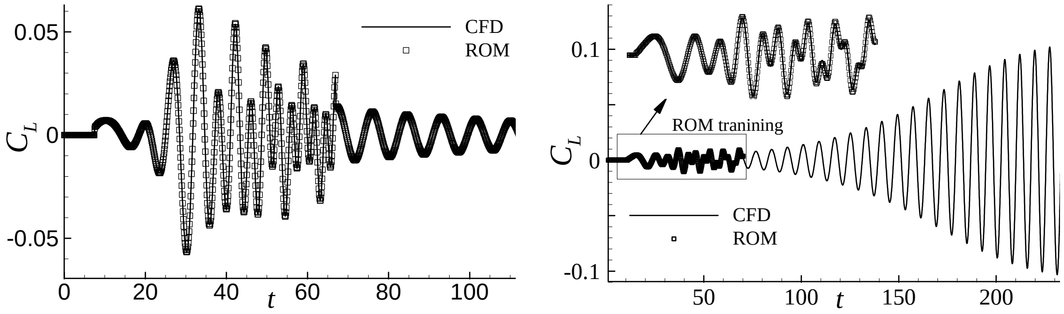

(a) *Re* = 45 (b) *Re* = 60

Fig.3. Identified results under the plunge training motion of circular cylinder

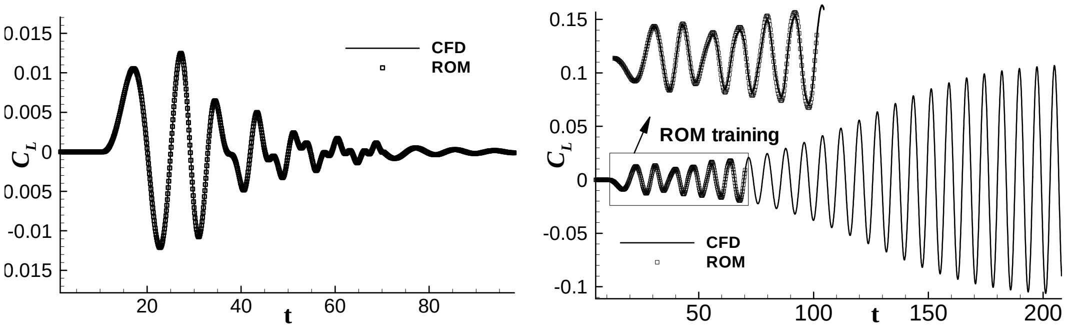

(a)*Re*=45 (b) *Re*=60

Fig.4. Identified results under the rotational training motion of circular cylinder

3.2 Identified results

Using the prepared input-output data from direct numerical simulations, linear ROMs are then constructed using the system identification method proposed in § 3.1. As an example, Identified results of $Re = 45$ and $Re = 60$ are shown in figs. 3 and 4. The delay orders are set to be *na*=*nb*=100 for high numerical accuracy.

It can be seen that the results predicted by ROMs agree well with those computed by the CFD solver at each Reynolds number, which shows that ROMs captured the dominant dynamics of both the stable and unstable flows past the cylinder at low Reynolds numbers.

3.3 Validation of the ROMs

In this section, the ROMs are validated in the time domain by comparing their harmonic forcing responses with that of full system in direct numerical simulations. The harmonic forcing signal is in the form as follow:

$$h = A\sin(2\pi F\, t) \qquad (7)$$

where A is the oscillation amplitude of cylinder and F is the reduced frequency of forced vibration.

Figs.5 and 6 present the time histories of C_L of a transversely oscillating cylinder predicted by ROM and CFD at two typical reduced frequencies $2\pi F = 0.5$ and $2\pi F = 0.8$. Figs.7 and 8 present the compared results of a rotationally oscillating cylinder. As can be seen, in the case of subcritical Reynolds number *Re*=45, the ROM predictions almost exactly match those calculated by the direct numerical simulations; On the other hand, in case of supercritical Reynolds number *Re*=60, the ROM also gives surprisingly good predictions for the initial development stage of the original system. As expected, for longer time, the growing amplitude of lift coefficient give rise to nonlinear dynamics and the solutions diverge to nonlinear limit-cycling states which are not captured by linear models.

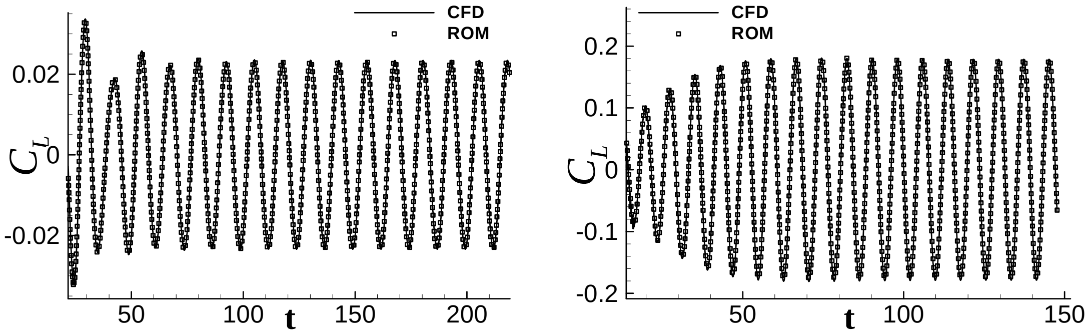

(a) $h = 0.025\sin(0.5t)$ (b) $h = 0.025\sin(0.8t)$

Fig.5. Comparisons of time responses of a transversely oscillating cylinder at *Re*=45

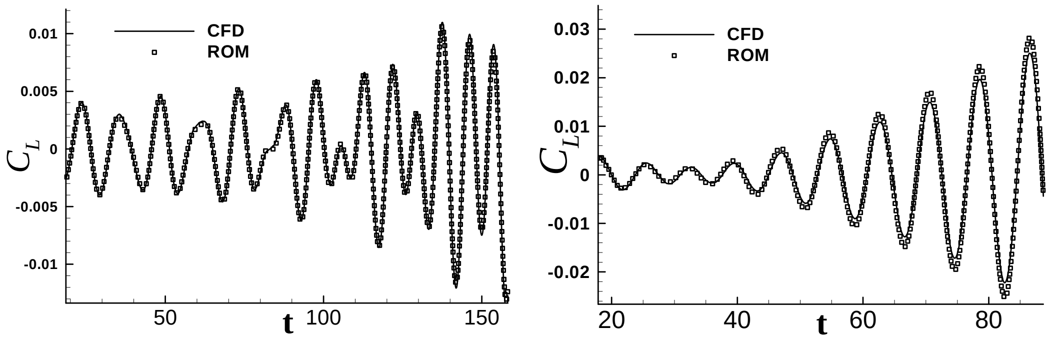

(a) $h = 0.001\sin(0.5t)$ (b) $h = 0.001\sin(0.8t)$

Fig.6. Comparisons of time responses of a transversely oscillating cylinder at *Re*=60

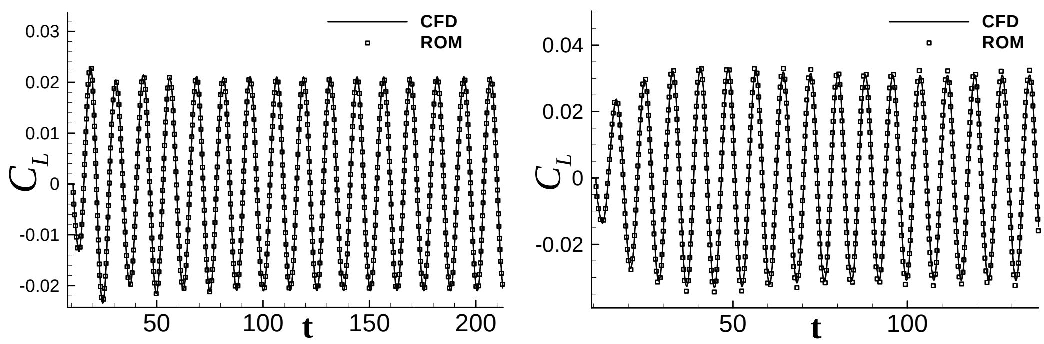

(a) $\alpha = 0.01\sin(0.5t)$ (b) $\alpha = 0.01\sin(0.8t)$

Fig.7. Comparisons of time responses of a rotationally oscillating cylinder at *Re*=45

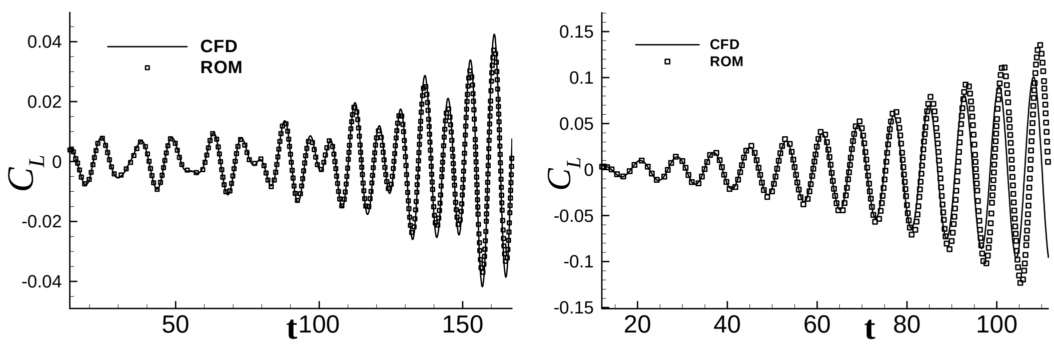

(a) $\alpha = 0.001\sin(0.5t)$ (b) $\alpha = 0.001\sin(0.8t)$

Fig.8. Comparisons of time responses of a rotationally oscillating cylinder at *Re*=60

4 Application to aeroelastic stability analysis

The focus of this paper is on constructing simple, linear aerodynamic models for the cylinder wake flow which are useful for aeroelastic stability analysis. With this in mind, the linear models are now tested by using them for aeroelastic stability analysis of an elastically-suspended cylinder at low Reynolds numbers.

4.1 ROM-based Aeroelastic Model

The cylinder is free to vibrate in the transverse direction. By defining a state vector $x_s = [h, \dot{h}]^T$, the cylinder motion equation (2) is then transformed into state-space form:

$$\begin{cases} \dot{x}_s(t) = A_s x_s(t) + qB_s y_a(t) \\ h(t) = C_s x_s(t) + qD_s y_a(t) \end{cases} \tag{8}$$

where:

$$A_s = \begin{bmatrix} 0 & 1 \\ -(2\pi F_n)^2 & -4\pi F_n \zeta \end{bmatrix}, \quad B_s = \begin{bmatrix} 0 \\ 1 \end{bmatrix}$$

$$C_s = \begin{bmatrix} 1 & 0 \end{bmatrix}, \quad D_s = \begin{bmatrix} 0 \end{bmatrix}, \quad q = \frac{2}{\pi M}$$

By defining the state vector $x_{as} = [x_s, x_a]$ and coupling the structural state equations (8) with aerodynamic state equations (6), we get the state equations and output equations for the coupled system as follows:

$$\dot{\boldsymbol{x}}_{FS}(t) = \boldsymbol{A}_{FS} \cdot \boldsymbol{x}_{FS}(t) \tag{9}$$

$$h(t) = \begin{bmatrix} \boldsymbol{C}_S & \boldsymbol{0} \end{bmatrix} \cdot \boldsymbol{x}_{FS}(t) \tag{10}$$

Where:

$$A_{as} = \begin{bmatrix} A_s + q \cdot B_s D_s C_s & q \cdot B_s C_a \\ B_a C_s & A_a \end{bmatrix}$$

Now, the ROM-based aeroelastic model for an elastically-suspended cylinder is found. The aeroelastic stability problem is then converted into solving and analyzing the eigenvalues of A_{as}. The real part of eigenvalue corresponds to the growth rate of eigenmode, while the imaginary part correspond to the circular frequency which is equal to 2π times the eigenfrequency of eigenmode.

4.2 Effect of natural frequency

The ROM-based aeroelastic model is now applied to the stability analysis of VIV at a subcritical Reynolds number $Re = 33$. The effect of natural frequency F_n on the stability characteristics of the aeroelastic system is studied in this section.

Fig. 9 shows the eigenvalues of the aeroelastic system varying with F_n at different mass ratios. There exist two neutral most unstable modes of interest: *"the nearly structural mode"*, renamed here structure mode, and the *von karmman mode*, renamed here wake mode. We can see that, the wake mode is absolutely stable at the subcritical *Re*=33. However, the interaction between the structure mode and the wake mode will eventually lead to the instability of the structure mode. It is shown that, as the reduced natural frequency F_n get close to 0.12 (the eigenfrequency of the von Karman mode), the root locus of the structure mode crosses the imaginary axis into the right half-plane, therefore the aeroelastic system will become unstable and the cylinder will undergoes self-excited oscillations. Generally, as the frequency is increased, the intensity of the oscillating increases to its maximum lever and then decreases. ROM-based aeroelastic model clearly shows that the occurring of vortex shedding at subcritical *Re* is essentially due to the instability of the structure mode.

The instability boundaries predicted by ROM-based model agree excellently well with that of the direct numerical simulation results. With $M = 50$ as an example, the two instability boundaries predicted by ROM-based model are $F_{n-lower} = 0.097$ and $F_{n-upper} = 0.147$. This is confirmed via direct numerical simulations shown in Fig.10 where the time responses at the vicinity of onset frequencies are compared. As can be seen, the time responses calculated by ROM-based aeroelastic model are in good agreement with that simulated by direct CFD/CSD method.

In addition, the effect of M on the instability boundaries is also investigated. From fig. 9(a) we can see that the range of the coupled frequency does not change with M . However, at low mass ratios, the instability boundaries of the aeroelastic system can be significantly affected by M , as shown in fig. 9(b). When $M > 50$, the instability boundaries rarely change with the mass ratio of the spring-mass system. This is most clearly shown in fig. 23 where the instability boundaries varying with M are plotted. Good agreement with that of Mittal et al. (2005) is observed.

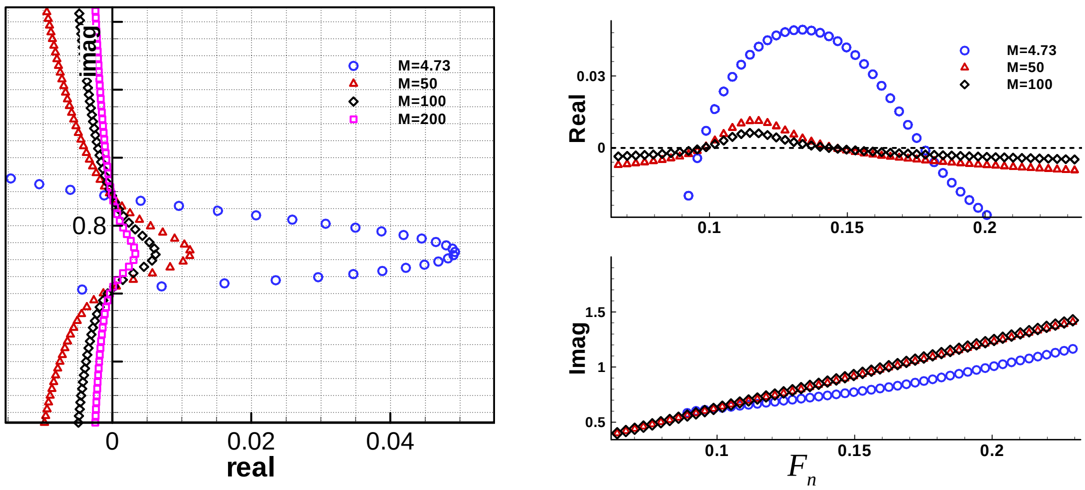

Fig.9. Root loci of the open-loop aeroelastic system at different mass ratios ($Re = 33$): (a) root loci versus the dimensionless frequency F_n ; (b) real part and imaginary part of the root loci.

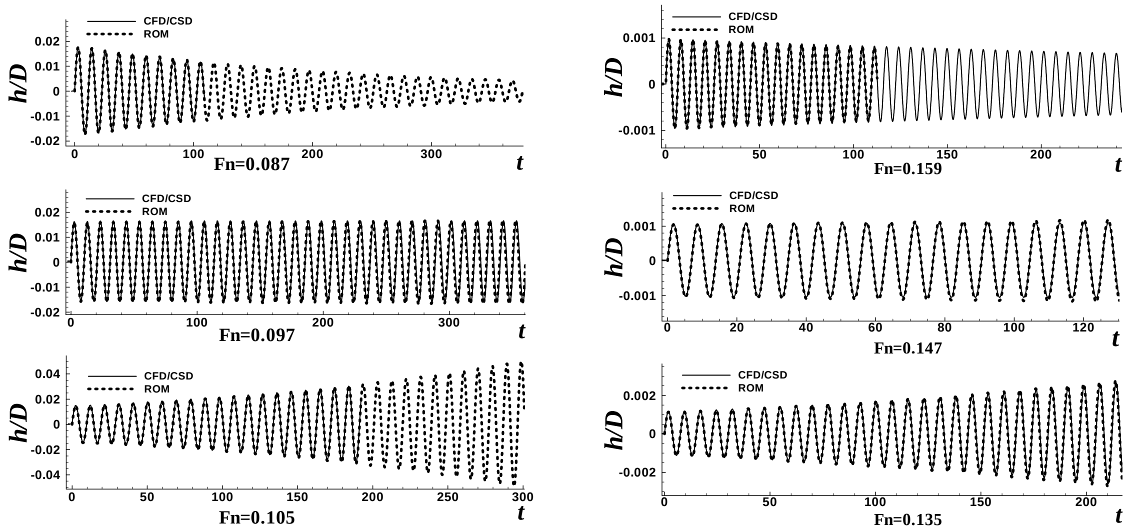

(a)The lower boundary (b) the upper boundary

Fig.10. Comparisons of the time responses at the vicinity of two instability boundaries ($M = 50$)

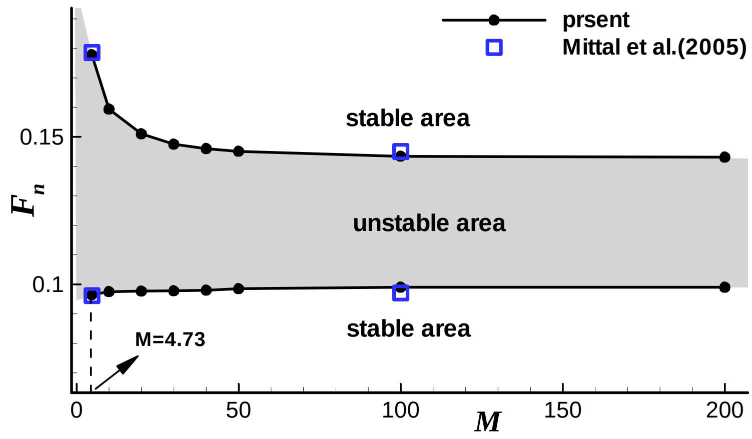

Fig.11. Instability boundaries versus the dimensionless mass ratio at $Re = 33$

4.2 Effect of Reynolds number

Reynolds number has a significant effect on the dynamics of the fluid flow and the aeroelastic system past a circular cylinder. Buffoni[17] found that vortex shedding could be triggered under subcritical conditions ($25 < Re < 49$) by transversely forced vibrations of the cylinder at specific frequencies. At lower Re, no vortex shedding is observed. Mittal et al. (2005) found that self-excited oscillations, accompanied by vortex shedding, are possible at Re as low as 20 through extensive numerical simulations.

Linear ROMs for several typical Reynolds numbers are constructed to investigate the effect of Re. Fig.12 shows the root loci of the aeroelastic system at various Re . And fig.13 shows the instability boundaries versus the Re for $M = 4.73$ and $M = 50$. We can see that the aeroelastic system is marginally stable at $Re \sim 20$. For $Re < 20$, no self-excited vibrations will be observed at all combinations of F_n and M , which is consistent with the results of Mittal et al. (2005) got by direct numerical simulations. However, the efficiency of ROM-based aeroelastic model is nearly 2 orders higher than that of numerical simulations.

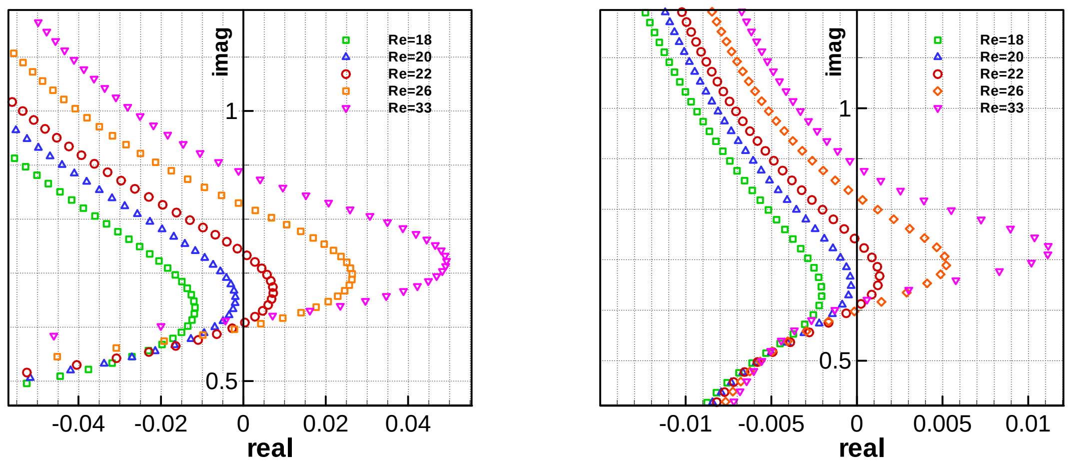

(a) $M = 4.73$ (b) $M = 50$

Fig.12. Root loci of the coupled aeroelastic system at different Re

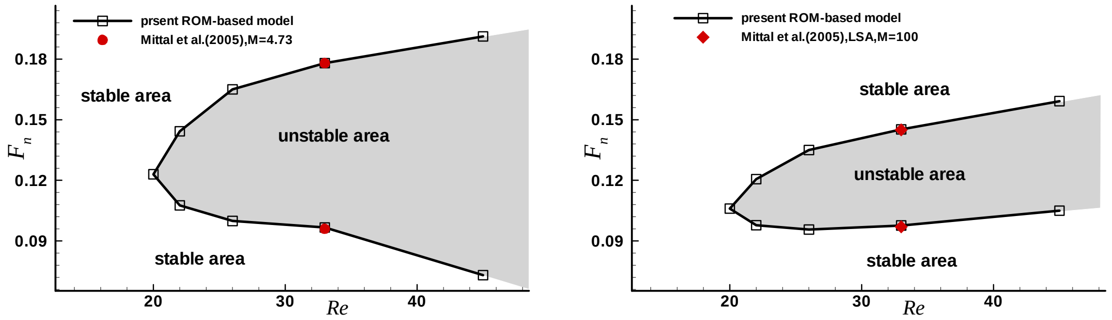

(a) $M = 4.73$ (b) $M = 50$

Fig.13. Instability boundaries varying with Re

5 Conclusions

This paper has focused on founding unsteady aerodynamic models for both the stable and unstable flows past a circular cylinder. From a practical point of view, these linear ROMs are useful for aeroelastic stability analysis and feedback controller design. For subcritical conditions ($Re < Re_{cr}$), the flow is absolutely stable, thus linear models can be identified directly using the input-output data based on the ARX model. While for supercritical conditions ($Re > Re_{cr}$), the unstable flow develops from a linear regime to finally nonlinear saturated state. Therefore, linear models for the unstable flow can be constructed by performing data training on the steady-state base flow in the linear regime.

The linear ROMs are then validated in the time domain by comparing their harmonic forcing responses to that of the direct numerical simulations. The results obtained by the linear models show excellent agreement with those calculated through direct numerical simulations. Moreover, the ROMs capture the dominant dynamics over the frequency where the unstable von Karman mode is found, which drives the design of a feedback controller. Therefore he models are capable for model-based controller design in future research.

Finally, the utility of linear models has been demonstrated most clearly by using them for aeroelastic stability analysis of an elastically-suspended cylinder at low Reynolds numbers. Once the ROM is constructed, the stability analysis of the aeroelastic system varying with F_n and M can be carried out expeditiously. The instability boundaries predicted by ROM-based aeroelastic model compared reasonably well to that of the direct numerical simulations and other's results, while the computational cost can be reduced by nearly 2 orders of magnitude.

The results indicate that the instability of the coupled aeroelastic system at subcritical Re_{cr} is due to the instability of the structure mode. Comparing the direct numerical method, linear models can provide great insight into the underlying mechanism of the occurring of vortex shedding as well as the frequency lock-in phenomenon in VIV.

References

[1] Williamson, C.H.K.. Vortex dynamics in the cylinder wake. *Annual Review of Fluid Mechanics* 28, 477–539, 1996.

[2] Sarpkaya, T. A critical review of the intrinsic nature of vortex-induced vibrations. *Journal of Fluids and Structures* 19, 389–447, 2004.

[3] Williamson, C.H.K., Govardhan, R.. Vortex-induced vibrations. *Annual Review of Fluid Mechanics* 36, 413–455, 2004.

[4] Bearman, P. W.. Circular cylinder wakes and vortex-induced vibrations. *Journal of Fluids and Structures* 27, 648–658, 2011.

[5] Cossu, C., Morino, L. On the instability of a spring-mounted circular cylinder in a viscous flow at low Reynolds numbers. *Journal of Fluids and Structures* 14, 183–196, 2000.

[6] Mittal, S., Singh, S. Vortex-induced vibrations at subcritical *Re*. *Journal of Fluids and Mechanics* 534, 185–194, 2005.

[7] Lucia, D.J., Beran, P.S., Silva, W.A. Reduced-order modeling: new approaches for computational physics. *Progress in Aerospace Sciences* 40, 51–117, 2004.
[8] Siegel, S.G., Seidel, J., Fagley, C., Luchtenburg, D.M., Cohen, K., McLaughlin, T. Low-dimensional modeling of a transient cylinder wake using double proper orthogonal decomposition. *Journal of Fluids and Mechanics* 610, 1–42, 2008.
[9] Graham, W.R., Peraire, J., Tang, K.Y. Optimal control of vortex shedding using low-order models. part i -open-loop model development. *International Journal for Numerical Method in Engineering* 44, 945–972, 1999.
[10] Noack, B.R., Pelivan, I., Tadmor, G., Morzynski, M. & Comte, P. Robust low-dimensional Galerkin models of natural and actuated flows. In Fourth Aeroacoustics Workshop. RWTH Aachen 26–27 Feb. 2004.
[11] Rowley, C.W., Juttijudata, V. Model-based control and estimation of cavity flow oscillations. In Proceedings of the 44th IEEE Conference on Decision and Control. Seville, Spain, 2005.
[12] Lumley, J. L., Blossey, P. Control of turbulence. *Annual Review of Fluid Mechanics* 30, 311–327, 1998.
[13] Prabhu, R.D., Collis, S.S., Chang, Y. The influence of control on proper orthogonal decomposition of wall-bounded turbulent flows. *Physics of Fluids* 12 (2), 520–537, 2001.
[14] Zhang, W.W., Ye, Z.Y. Control Law Design for Transonic Aeroservoelasticity. *Aerospace Science and Technology* 11, 136-145, 2007.
[15] Illingworth, S. J., Morgans, A. S., & Rowley, C. W. Feedback control of cavity flow oscillations using simple linear models. *J. Fluid Mech.* 709, 223–248, 2012.
[16] Zhang, W., Jiang, Y., & Ye, Z. Two better loosely coupled solution algorithms of CFD based aeroelastic simulation. *Eng. Appl. Comp. Fluid.* 1(4), 253–262, 2007.
[17] Buffoni, E. Vortex shedding in subcritical conditions. *Physics of Fluids* 15, 814-816, 2003.

Contact Author Email Address

Li454181405@126.com

Copyright Statement